http://ansinet.com/itj

ITJ

ISSN 1812-5638

INFORMATION TECHNOLOGY JOURNAL

ANSInet
Asian Network for Scientific Information
308 Lasani Town, Sargodha Road, Faisalabad - Pakistan

Information Technology Journal 12 (24): 8446-8453, 2013
ISSN 1812-5638 / DOI: 10.3923/itj.2013.8446.8453

Anti-jam Adaptive Array Instrument for the Weak Gnss in the Fast Time-varyimg Scenario

[1,2]Zhang Yanjun and [1]Li Ping
[1]School of Mechatronical Engineering, Beijing institute of technology, 100081, Beijing, People's Republic of China
[2]National Key Laboratory for Electronic Measurement Technology, North University of China, 030051, Taiyuan, People's Republic of China

Abstract: The article introduced the structure and technology method of the anti-jam instrument based on the adaptive arrays theory for the weak GNSS. The different algorithms is transformed into the uniform GSC program structure which can contribute to saving hardware cost and improving the code's efficiency. To meet the need of the fast time-varying scenario, the multistage Wiener filter is introduced. Analysis and numerical experiments show that it is an effective method, especially in the fast time-varying scenario.

Key words: Adaptive arrays, STAP, multistage wiener filter

INTRODUCTION

The anti-jamming technology of adaptive array has been widely applied to the fields of communication, navigation, radar and sonar, etc and so on. James, D.M. summarizes an overview of the adaptive antenna array up to the end of 1985 and list a majority of open-literature bibliography of the field(Mass, 1986; Van-Veen and Buckley, 1988) introduces beamforming approaches to spatial filtering from a signal processing perspective.

Capon beamforming algorithm could keep the output power of array to minimum in under the guarantee of the desired signal without distortion (Capon, 1969). Then Frost extended the beamforming technology to multiple linear constraints from single direction constraint and meanwhile he presented the space-time architecture of the algorithm (Frost, 1972). As an alternative approach, the Generalized Sidelobe Canceling (GSC) structure is described by Griffiths (Griffiths and Jim, 1982). To suppress the broadband interference, the Space Time Adaptive Processing (STAP) structure can be applied. Then, the nulling bandwidth performance of adaptive linear arrays with up to 10 elements is discussed which is affected by the number of taps in the delay lines and the amount of delay between taps (Vook and Compton, 1992). As one of the most important application areas, Global Navigation Satellite System (GNSS) array anti-interference technology has also been developed greatly and is still in research at present. GNSS signal is extremely weak when it arrived to the receiver 's antenna and the typical power value of the GPS C/A code is -160 dBw (environmental temperature: 290 K), about 20 dB below the thermal noise.

The anti-jam technology of STAP applied to GPS has been researched from the late 1990s,and references (Hatke, 1998) gives a introduction on how STAP beamformer is designed for GPS nulling the jamming in a severe nearfield multipath environment. Subsequently, Fante made a relatively complete discussion about anti-jam GPS receivers based on STAP (Fante and Vaccaro, 2000)

With the in-depth study of the adaptive array theory and rapid advancement in electronics, many kinds of anti-jam array instrument for GNSS have been designed and developed.

Rockwell Collins Inc shows its long GPS Anti-Jam history and presents its Digital AJ Products whose adaptive filter options include STAP and SFAP technology(Carlson *et al*., 2003, Rowe *et al*., 2005).

In this study, the author designs a kind of STAP array anti-jam instrument architecture in practice applications for narrowband and wideband blanket interference. It makes the Generalized Sidelobe Canceling (GSC) structure as an unified platform for adaptive array signal processing algorithm and equivalently realizes the Minimum Variance Distortionless Response (MVDR) algorithm for known desired direction and Power (PI) Inversion algorithm for unknown desired direction.

Corresponding Author: Zhang Yanjun, School of Mechatronical Engineering, Beijing institute of technology, 100081, Beijing, People's Republic of China

As a result, the same system architecture can fit different application environmental requirements by different work mode. The instrument module enhance its cohesiveness and independence and can be controlled by the passed parameters.

But in the fast time-varying interference scenarios, the above algorithm cannot meet the real-time requirement and the anti-jamming performance will drop greatly. To solve this problem, the Modified Multistage Wiener Filter (MSWF) reduced-rank algorithm is applied to the unified GSC structure. Although the anti-jam performance remains the same basically, the computational complexity is reduced rapidly for avoiding the operation of matrix inversion.

THEORETICAL FOUNDATION

Algorithm transformation from MVDR to GSC: Assume that there are M omnidirectional antenna array elements and each element contains N successive samples. The input vector is written as: $X(k) = [x_{11}, x_{12}, \ldots, x_{1N}, \ldots, x_{M1}, X_{M2}, \ldots, x_{MN}]$ the steering vector of the desired signal is represented by $\vec{a}$ and the weight vector is represented by W. Under the rule of MVDR.

The weight vector W is the solution to the following equation, $W = [w_{11}, w_{12}, \ldots, w_{1N}, \ldots, w_{M1}, w_{M2}, \ldots, w_{MN}]^H$:

$$\begin{cases} \min Pout = \min\ E\{|y(k)|^2\} = \min E(W^H R_x W) \\ \text{st. } W^H \vec{a} = 1 \end{cases} \quad (1)$$

By the method of Lagrange Multipliers, the constrained optimization W is given by:

$$W_{MVDR} = \frac{R_x^{-1} * \vec{a}}{\vec{a}^H * R_x^{-1} * \vec{a}} \ldots\ldots \quad (2)$$

where, R is the covariance matrix computed by the observational data vector X(k) and must be a non-singular matrix.

Then, let $\vec{h}_0 = \vec{a}/\|\vec{a}\|$, W_{MVDR} is given by:

$$W_{MVDR} = \frac{R_x^{-1} * \vec{a}}{\vec{a}^H * R_x^{-1} * \vec{a}} = \frac{R_x^{-1} * \vec{h}_0 * \|\vec{a}\|}{\vec{h}_0^H * R_x^{-1} * \vec{h}_0 * \|\vec{a}\|^2} \quad (3)$$

Let $W_{MVDR1} = W_{MVDR} * \|\vec{a}\|^2$ which cannot change the rate of input SNR to output SNR, the following equation is given:

$$W_{MVDR} = \frac{R_x^{-1} * \vec{h}}{\vec{h}_0^H * R_x^{-1} * \vec{h}} = \frac{T^H * (T * R_x * T^H)^{-1} * (T * \vec{h}_0)}{\vec{h}_0^H * T^H * (T * R_x T^H)^{-1} * (T * \vec{h}_0)} \quad (4)$$

(is a non-singular matrix, indicating $T \neq 0$). Let:

$$T = \begin{bmatrix} \vec{h}_0^H \\ B_0 \end{bmatrix}$$

and $B_0 = \text{null}(\vec{h}_0)$, then $B_0 * \vec{h}_0 = 0$. Let $\vec{e} = T * \vec{h}_0$, the solution is given by:

$$\vec{e} = [1\ 0 \ldots \ldots 0]^T \quad (5)$$

Substituting Eq. 5 into 4, we have:

$$W_{MVDR1} = \frac{T^H * (T * R_x * T^H)^{-1} * \vec{e}}{\vec{h}_0^H * T^H * (T * R_x * T^H)^{-1} * \vec{e}} \quad (6)$$

Because of:

$$T = \begin{bmatrix} \vec{h}_0^H \\ B_0 \end{bmatrix}$$

Eq. 7 can be obtained:

$$T * X = \begin{bmatrix} h_0^H \\ B_0 \end{bmatrix} * X = \begin{bmatrix} d_0 \\ X_0 \end{bmatrix} \quad (7)$$

The following expression is was derived from Eq. 7:

$$\begin{aligned} &T * R_X * T^H = T * E(X * X^H) * T^H = E((T * X) * (T * X)^H) \\ &= E\left(\begin{bmatrix} d_0 \\ X_0 \end{bmatrix} * [d_0^*\ X_0^H]\right) = E\begin{bmatrix} d_0 * d_0^* & d_0 * X_0^H \\ X_0 * d_0^* & X_0 * X_0^H \end{bmatrix} = \begin{bmatrix} \sigma_{d_0}^2 & r_{X_0 d_0}^H \\ r_{X_0 d_0} & RX_0 \end{bmatrix} \end{aligned} \quad (8)$$

Then the inverse of the matrix $TR_X T^H$ is obtained:

$$\begin{aligned} &(T * R_X * T^H)^{-1} = \begin{bmatrix} \sigma_{d_0}^2 & r_{X_0 d_0}^H \\ r_{X_0 d_0} & R_{X_0} \end{bmatrix}^{-1} = \\ &\begin{bmatrix} 1 & -r_{X_0 d_0}^H * R_{x_0}^{-1} \\ -R_{x_0}^{-1} * r_{X_0 d_0} & \xi_0 * R_{X_0}^{-1} + \xi_0 + R_{X_0}^{-1} r_{X_0 d_0} r_{X_0 d_0}^H R_{X_0}^{-1} \end{bmatrix} \xi_0^{-1} \end{aligned} \quad (9)$$

From Eq. 5 and 9, the following expression is given:

$$(T * R_X * T^H)^{-1} * \vec{e} = \begin{bmatrix} 1 \\ -R_{x_0}^{-1} * r_{X_0 d_0} \end{bmatrix} * \xi_0^{-1} \quad (10)$$

Substituting Eq. 10 into 6, W_{MVDR1} is computed to be:

$$W_{MVDR1} = \frac{T^H * \xi_0^{-1}\begin{bmatrix}1\\ -R_{x_0}^{-1} * r_{X_0 d_0}\end{bmatrix}}{(T*\vec{h})^H ** \xi_0^{-1} * \begin{bmatrix}1\\ -R_{x_0}^{-1} * r_{X_0 d_0}\end{bmatrix}} = T^H * \begin{bmatrix}1\\ -R_{x_0}^{-1} * r_{X_0 d_0}\end{bmatrix}$$

$$= [\vec{h}_0 \ B_0^H] * \begin{bmatrix}1\\ -R_{x_0}^{-1} * r_{X_0 d_0}\end{bmatrix} = \vec{h}_0 - B_0^H * -R_{x_0}^{-1} * r_{X_0 d_0} \quad (11)$$

And the output y(k) is determined by:

$$y(k) = W^H_{MVDR1} * X(k) \quad (12)$$

For GSC algorithm, when $\vec{h}_0 = \vec{a}/\|\vec{a}\|$ ($\vec{a}$ still represents steering vector of the desired signal) and the block matrix $B_0 = \text{null}(\vec{h}_0)$, the structure is described by Fig. 1.

The output error signal $\varepsilon_0(k)$ is the result of the algorithm and it equals the array output signal y(k):

$$\varepsilon_0(k) = d_0(k) - \hat{d_0}(k) = h_0^H * X(k) - W_{X_0}^H * X_0(k) = h_0^H * X(k)$$
$$-W_{X_0}^H * B_0 * X(k) = (h_0^H - W_{X_0}^H * B_0) * X(k) = W_{GSC}^H * X(k)$$

That is:

$$W_{GSC} = \vec{h}_0 - B_0^H - W_{X_0} \quad (13)$$

According to Wiener optimal design criterion, the solution of the W_{X_0} s given by:

$$W_{X_0} = R_{X_0}^{-1} * r_{X_0 d_0} \quad (14)$$

Then, substituting Eq. 14 into 13, we have:

$$W_{GSC} = \vec{h}_0 - B_0^H - R_{X_0}^{-1} * r_{X_0 d_0} \quad (15)$$

So, from Eq. 11 and 15, the following equation is true:

$$W_{GSC} = W_{MVDR1} \quad (16)$$

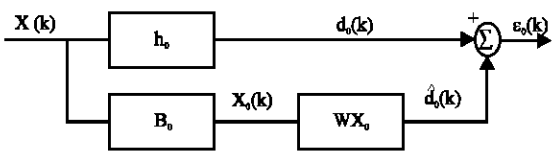

Fig. 1: GSC algorithm structure

From Eq. 16, we can transform the MVDR into the GSC equivalently and establish the mathematical method for the next reduced-rank operation.

Algorithm transformation from PI to GSC: As the introduction have mentioned before, GNSS signal is extremely weak when it arrived to the receiver's antenna, even 20~30 dB lower than in the receiver noise. For this particular property, the Power Inversion blind adaptive algorithm is an appropriate choice.

The PI algorithm is described by the following constraints:

$$\begin{cases}\text{Minimum(pout)} = E\{|\ y(k)\ |^2\} = E(W^H R_x W)\\ \text{st.} W^H \vec{\alpha} = 1\\ \vec{\alpha} = [1, 0, 0, \ldots 0]^T\end{cases} \quad (17)$$

Compared with the (1), the weight vector is described by

$$W = [1, w_{21}, \ldots, w_{2N}, \ldots, w_{M1}, \ldots, w_{MN}]^H$$

That is to say, the first array element is appointed to be the reference signal and its weight coefficient equals 1. By adjusting the rest of weighting vector W, the Mean Square Error (MSE) between array element 2¡«M and the first array element can reach the minimum value.

Hence, the optimum solution for Eq. 17 is converted to the following unconstrained optimization problem:

$$\begin{aligned}&\text{Pout} = E\{|\ y(k)\ |^2\} = E\{|\ x_1(k) + w_{21}x_2(k) + \ldots + \ldots w_{2N}x_2\\ &(k-N+1) + \ldots + w_{M1}x_M(k) + \ldots + w_{MN}x_M(k-N+1)|^2\}\\ &= E\{|\ x_1(k) + W^H X_0(k)\ |^2\}\\ &= E\{x_1(k)x^*_1(k) + W^H X_0(k)x^*_1(k) + X_1(k)X_0{}^H(k)\\ &W + W^H X_0(k)X_0{}^H(k)W\}\\ &= r_{x1}(k)x_1(k) + W^H Rx_0(k)x_1(k) + W^H Rx_0(k)X_0(k)W\end{aligned} \quad (18)$$

where, $X_0(k) = [x_{21}, \ldots, x_{2N}, \ldots, x_{M1}, x_{M2}, \ldots, x_{MN}]$. To take the derivative of Eq. 15 with respect to:

$$\partial P_{out} / \partial W = Rx_0(k)x_1(k) + Rx_0(k)x(k)W$$

Let $\partial P_{out} / \partial W = 0$ and to solve the equation, we know that when:

$$W = -Rx_0^{-1}(k)x(k)Rx_0(k)x_1(k) \quad (19)$$

the minimum value of P_{out} can be gained. Then the optimal weight vector:

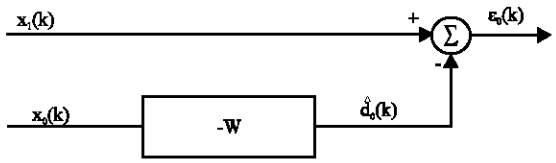

Fig. 2: PI algorithm structure

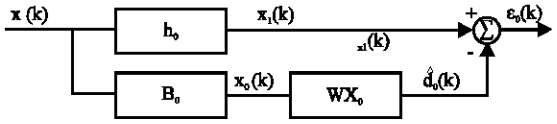

Fig. 3: Transformation of PI algorithm into GSC algorithm structure

$$W_{pi} = [1 - R^{-1}x_0(k)x(k)Rx_0(k)x_1(k)]^T \quad (20)$$

The structure of the PI algorithm is described by Fig. 2.

From Fig. 2, we know that the PI algorithm essentially is the implement of the classic Wiener filter. Similar to the Fig.1, the structure of the PI algorithm can be transformed to that of the GSC which is shown in Fig. 3.

where, $X(k) = [x_1(k)\ X_0(k)^T]^T$:

$$h_0^{\rightarrow} = [10...0]^T x_1(k) = h_0^H * x(k) = d_0(k)$$

$$B_0 = \begin{bmatrix} 0\,1\,0\ \ldots\ 0 \\ 0\,0\,1\ \ldots\ 0 \\ \ldots\ \ldots\ \ldots\ \ldots\ \ldots \\ 0\ 0\ 0\ 0\ 0 \end{bmatrix}$$

$$(M-1)N \times ((M-1)N+1)x_0(k) = B_0 * x(k)$$

Then:

$$W_{x0} = -R^{-1}x_0\gamma x_0 d_0 \quad (21)$$

From Fig. 3 and Eq. 21, the PI algorithm is exactly equivalent to the GSC algorithm by adding a few auxiliary operations.

WORKING PRINCIPLE OF THE INSTRUMENT

Figure 4 shows a block diagram of *i*-array element space-time anti-jam instrument architecture. The antenna array receives the signal on separate antenna elements. By the front-end circuit, the signal is downconverted to an intermediate frequency sufficient for processing by the subsequent circuit. Then the A/D converter transforms the signal into the digital domain. The digital data is divided into two branches. One is orthogonally demodulated by multiplying the local carrier and is removed high-frequency component by the lowpass digital filter. The frequency of the local carrier is controlled by the Frequency Control Word(FCW)which is passed by the next functional module. Then after demodulation the I & Q signal form a complex variable I+j*Q,which is the baseband signal for the next STAP operation. Another branch data flows into the sample data block memory which is realized via Static Random Access Memory (SRAM). After a period of storage time, the sample data block is read out and also demodulated into I+j*Q in the same way. The DSP module uses these data to compute the weight coefficients W according to the above algorithm in the section.

The IMU(Inertial Measurement Unit) in Fig. 4 can supply the carrier own attitude information to the DSP over the 1553-B bus. The satellite ephemeris data is also transferred by the 1553B bus which is stored in the subsequent GNSS receive module. With the known ephemeris data and the platform own attitude data, DSP can calculate the desired direction vector and executes the GSC algorithm based on MVDR. If the ephemeris data is unavailable, DSP executes the GSC algorithm based on PI. The instruction word is sent by the Bus Controller(BC) connected to the 1553B bus.

Then, DSP sends the adaptive weights to FPGA, where the STAP is executed and the output signal:

$$Y(k) = W^H X(k)$$

Note that the weights is computed using the data sampled during the previous time period and the present data sampled is used for the next time period computing. To high speed data acquisition, it has little effect on the output result.

Finally, after interference suppression the baseband data is adjusted to output by digital AGC.

In order to demonstrate the performance of the common platform of the GSC structure implemented by MVDR and PI, the simulation is made for 6 uniform circular array elements with one GPS satellite signal and two kinds of interference. The simulation parameters is shown in Table 1.

In the Table 1, LFM1[1] is linear frequency-modulated continuous wave. LFM2[2] is linear frequency-modulated periodic wave and the period T equals 3(during 1ms period).

Figure 5 and Figure 6 depict the antenna pattern for the desired direction angle (50, 30°) in MVDR algorithm

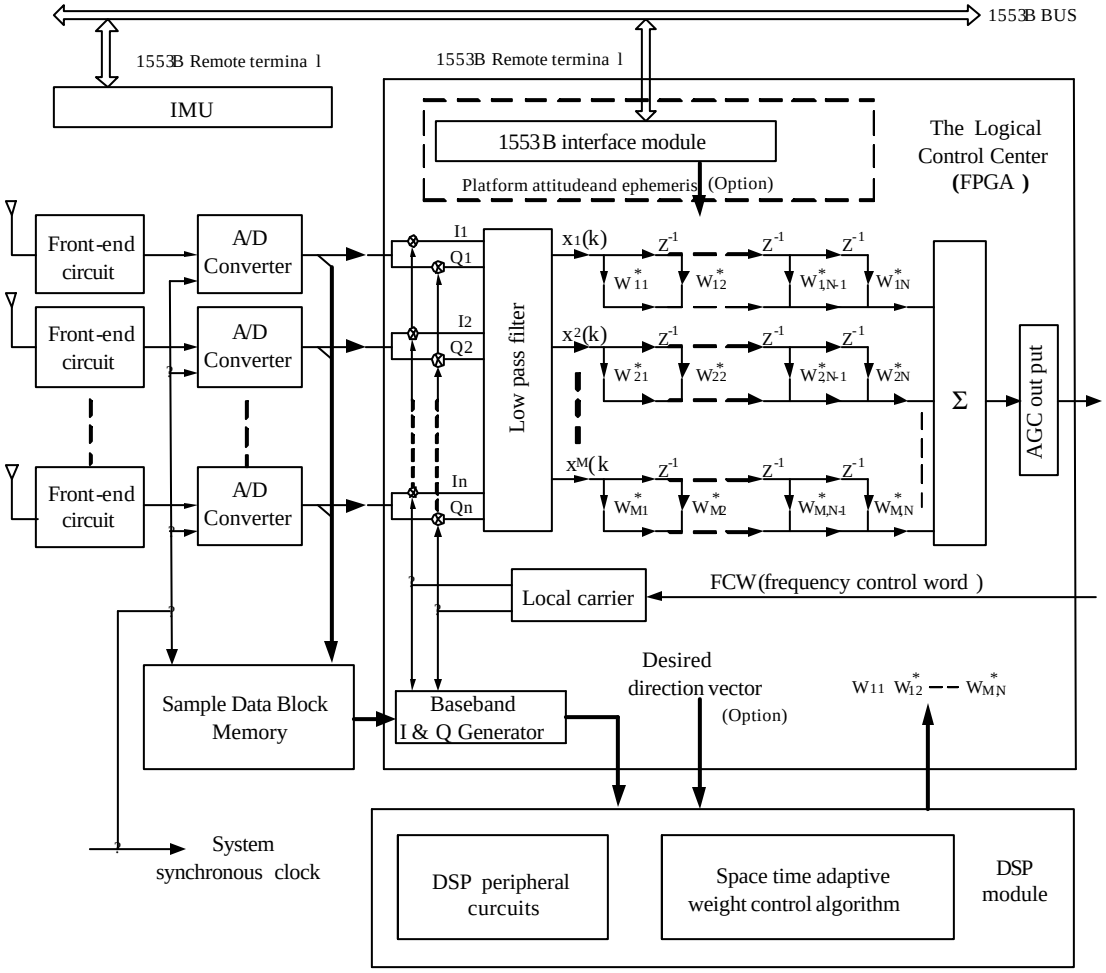

Fig. 4: Block diagram of i-array elements

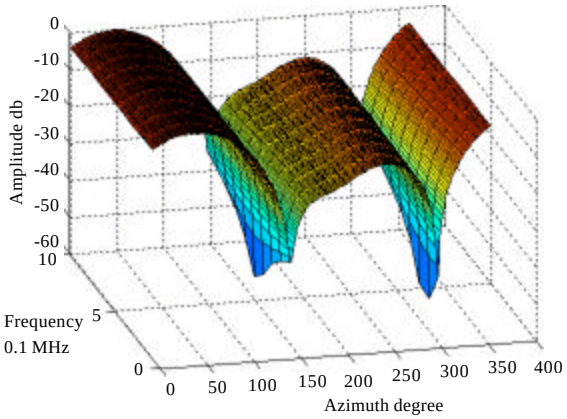

Fig. 5: Antenna pattern of 6 UCA with 10 delay taps for the GNSS signal

and Fig. 7 and 8 depict the antenna pattern for the interference direction angle(150°,40°) in PI algorithm.

From the figures we can know that the MVDR can get the maximum value in a desired direction and PI can only null the interference with a small loss of the signal. So the MVDR can get a higher SJNR than PI. But both the algorithm can achieve the required SJNR value for C/A acquisition. For example, the SJNR is about -19 dB for PI algorithm in the simulation.

FAST ALGORITHM APPLICATION

Figure 5-8 show that the simulation result can meet the requirements of Table 1. The weight coefficients is calculated by Sample Matrix Inversion (SMI). But in reality the algorithm would not appear to be a very

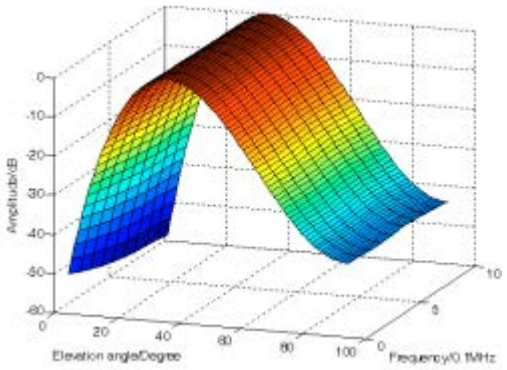

Fig. 6: Antenna pattern of 6 UCA with 10 delay taps for one signal and two interference

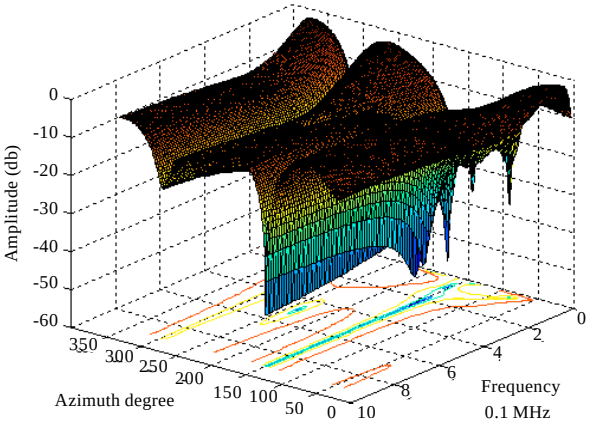

Fig. 7: Antenna pattern of 6 UCA with 10 delay taps for the GNSS signal

Table 1: Simulation parameter

Signal type	GPS	LFM1[1]	LFM2[2]
Carrier center frequency(MHz)	1575	1575	1575
Bandwidth (MHz)	2	2	2
Azimuth (Degree)	50	150	300
Elevation (Degree)	30	40	60
Input SNR/SJR (dB)	-20	-52	-58

practical method, especially in the fast time-varying scenario. In references (Goldstein *et al.*, 1998),the Multistage Wiener Filter (MWF) is introduced to solve this problem.

On the basis of the GSC structure in Fig. 3, the first stage of the decomposition is shown in Fig. 9.

According to Wiener optimal design criterion, the equation is established as follows:

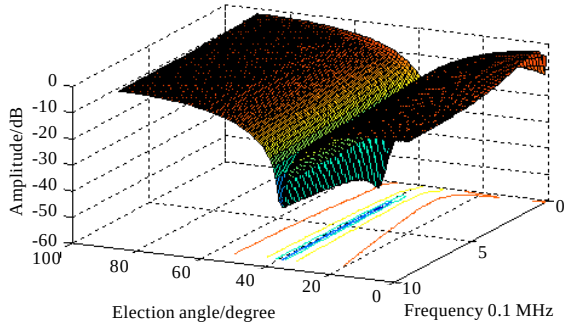

Fig. 8: Antenna pattern of 6 UCA with 10 delay Taps for the GNSS signal

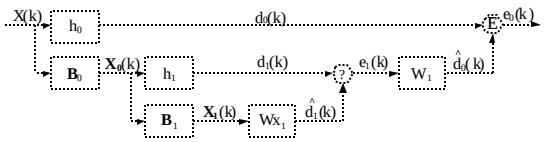

Fig. 9: ?????????

$$W_{x1} = R_{X_1}^{-1} r_{x_1 d_1} \ldots\ldots \tag{22}$$

The Minimum Mean Square Error (MMSE) of the $\varepsilon_1(k)$ is computed to be:

$$\begin{aligned} &E(\|\varepsilon_1(k)\|\min^2) = E(\|d_1(k) - \hat{d_1(k)}\|^2) = E(\|d_1(k) - W_{X_1}^H X_1(k)\|^2) \\ &= E((d_1(k) - W_{X_1}^H X_1(k))(d_1(k) - W_{X_1}^H X_1(k))^*) \\ &= E(d_1(k) d_1^*(k)) - (d_1(k) X_1^H(k) W_{X_1} + W_{X_1}^H X_1(k) d_1^*(k)) + \\ &W_{X_1}^H X_1(k) X_1^*(k) W_{X_1}) \end{aligned} \tag{23}$$

To plug Eq. 22 into 23, the MMSE is calculated by Eq. 2:

$$\begin{aligned} &E(\|\varepsilon_1(k)\|_{\min}^2) \\ &= E(d_1(k) d_1^*(k)) - E(d_1(k) X_1^H(k)) R_{X_1}^{-1} r_{X_1 d_1} - r_{X_1 d_1}^H \\ &(R_{X_1}^{-1})^H E(X_1(k)) d_1^*(k)) + r_{X_1 d_1}^H (R_{X_1}^{-1})^H R_{X_1} R_{X_1}^{-1} r_{X_1 d_1} \\ &= E(d_1(k) d_1^*(k)) - E(d_1(k) X_1^H(k)) R_{X_1}^{-1} r_{X_1 d_1} \\ &- r_{X_1 d_1}^H (R_{X_1}^{-1})^H r_{X_1 d_1} + r_{X_1 d_1}^H (R_{X_1}^{-1})^H r_{X_1 d_1} \\ &= E(d_1(k) d_1^*(k)) - r_{X_1 d_1}^H R_{X_1}^{-1} r_{X_1 d_1} \\ &= \sigma_{d_1}^2 - r_{X_1 d_1}^H R_{X_1}^{-1} r_{X_1 d_1} \end{aligned} \tag{24}$$

We continue to calculate W_1 by Wiener criterion, the Eq. 25 is established:

$$W_1 = R_{\varepsilon_1}^{-1} r_{\varepsilon_1 d_0} \ldots. \tag{25}$$

According to Eq. 24, the R_{ε_1} and $r_{\varepsilon_1 d_0}$ is given by:

$$\begin{aligned} R\varepsilon_1 &= E(\varepsilon_1(k) * \varepsilon_1^*(k)) = E(\| \varepsilon_1(k) \|_{min}^2) \\ &= \sigma_{d1}^2 - r_{X_1 d_1}^H R_{X_1}^{-1} r_{X_1 d_1} \\ r_{\varepsilon_1 d_0} &= E(\varepsilon_1(k) d_0^*(k)) \\ &= E((d1(k) - W_{X_1}^H X_1(k) d_0^*(k)) \\ &= E((d_1(k) d_0^*(k) - W_{X_1}^H X_1(k) d_0^*(k)) \\ E((d_1(k) d_0^*(k)) &= E((h_1^{\vec{H}} * X_0(k) * d_0^*(k)) \end{aligned} \tag{26}$$

$$\begin{aligned} r_{\varepsilon 1 d_0} &= FE(\varepsilon_1(k) d_0^*(k)) \\ &= E((d_1(k) - W_{X_1}^H X_1(k)) d_0^{\delta}(k)) \\ &= E((d_1(k) d_0^*(k) - W_{X_1}^H X_1(k) d_0^{\delta}(k)) \\ &= E((d_1(k) d_0^*(k)) = E((h_1^{\vec{H}} * X_0(k) * d_0^*(k))) \\ &= h_1^{\vec{H}} * E(X_0(k) * d_0^*(k)) = h_1^{\vec{H}} * rX_0 d_0 \end{aligned} \tag{27}$$

Then, the final output error is expressed by:

$$\begin{aligned} \varepsilon_0(k) &= d_0(k) - W_1^* \varepsilon_1(k) = d_0(k) = W_1^*(d_1(k) - \bar{d}_0(k)) \\ &= d_0(k) - W_1^*(d_1(k) - W_{X_1}^H X_1(k)) \\ &= d_0(k) - [W_1^* - W_1^* W_{X_1}^H] \begin{bmatrix} d_1 & (k) \\ X_1 & (k) \end{bmatrix} \\ &= d_0(k) - W_d^H T X_0(k) = d_0(k) - (T^H W_d)^H X_0(k) \end{aligned} \tag{28}$$

Under the condition of equal ε_0 (k) the weight coefficient in Fig. 3 and the one in Fig. 10 are equivalent. Then:

$$W_{X_0} = T^H W_d \tag{29}$$

and:

$$T = \begin{bmatrix} h_1^H \\ B_1 \end{bmatrix}, W_d = [W_1 - W_1 W_{X1}]$$

$X_0(k)$ in Fig. 10 can be decomposed further in the same way until it becomes a scalar, not a vector. Then:

$$T = \left[h_1^{\vec{H}} \; h_2^{\vec{H}} B_1 \ldots h_{N-1}^{\vec{H}} \prod_{k=N-2}^{1} B_k \prod_{k=N-1}^{1} B_k \right]^T$$

$$W_d = \left[W_1 - W_1 W_2 \ldots . (-1)^{N-1} \prod_{k=1}^{N-1} W_k \right]$$

finally:

$$W_{X0} = T^H W_d \tag{30}$$

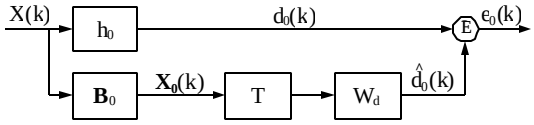

Fig. 10: ????????

Because the vector X(k) has been decomposed the scalar, the inversion of the autocorrelation matrix is avoided. In the practical engineering calculations, the matrix inversion is the bottleneck of computation. However, we can avoid it utilizing the MWF algorithm without impacting performance.

To improve the calculation efficiency, the blocked matrix has been modified according to references (Ricks and Goldstein, 2000).

$$\begin{aligned} X_o(k) &= X(k) - \vec{h_0} * d_0(k) = X(k) - \vec{h_0} * (\vec{h_0^H} X(k)) \\ &= X(k) * \vec{h_0} * \vec{h_0^H} X(k) = (I - \vec{h_0} * \vec{h_0^H}) X(k) \end{aligned} \tag{31}$$

Where:

$$\vec{h_0} = \vec{\alpha} / \| \vec{\alpha} \|$$

and let:

$$B_0 = P - \vec{h_0} * \vec{h_0^H}$$

Then:

$$X_0(k) = (I - \vec{h_0} * \vec{h_0^H}) X(k) \tag{32}$$

Similarly:

$$B_1 = I - \vec{h_1} * \vec{h_1^H}$$

$$X_1(k) = (I - \vec{h_1} * \vec{h_1^H}) X_0(k) \tag{33}$$

The References (Honig and Xiao, 2001; Honig and Goldstein, 2002) give discussion of reduced-rank performance about the MWF. In the same scene as Table 1, the algorithm described by (33) is simulated for the 1ms sample data(one C/A period) in the same sample frequency (60 MHz). The simulation result is shown in Fig. 11. It indicate that the STNR out performance is a function of MWF rank and can achieve full rank result when the rank is greater than 5.

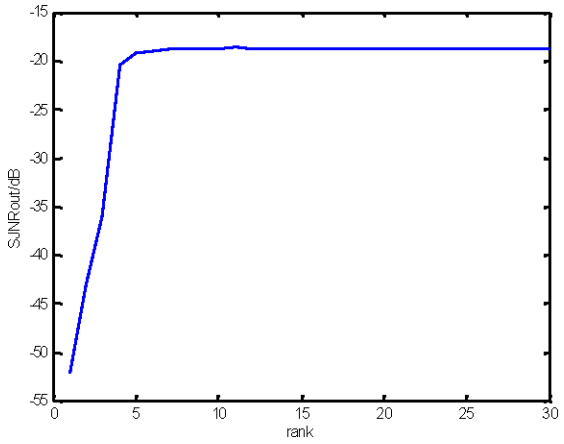

Fig. 11: SJNRout of the array by the MWF algorithm

If the number of multiplications is used as the main indicator to measure the time complexity, the computation of the Sample Matrix Inversion (SMI) is $O(MN)^3$ (M is the number of the array, N is the number of the time delay tap)and the computation is $O(MN)^2$ in $X_{i-1}(k) = B_{i-1}*X_i(k)$, the modified MWF computation is O(MN) in:

$$X_{i-1}(k) = (I - \overrightarrow{h_1} * \overrightarrow{h_1^H}) X_i(k)$$

Thus, it can be seen that the modified MWF algorithm can adapt to the fast time-varying scenario than the other two algorithms.

CONCLUSION

A kind of anti-jam instrument architecture is presented which uses adaptive array technology to resist suppressing jamming for receiving the weak GNSS signal. It have a shared algorithm structure to adapt to different situations. The improved MWF is applied in order to reduce the calculation burden in the fast time-varying scenario. In the practical application, it is easy to add flash memory chips capable of storing hundreds of megabytes of data in Fig. 4. Thus we have enough sample data to evaluate the effectiveness of the algorithm.

REFERENCES

Capon, J., 1969. High-resolution frequency-wavenumber spectrum analysis. Proc. IEEE., 57: 1408-1418.

Carlson, S.G., C.A. Popeck, M.H. Stockmaster and C.E. McDowell, 2003. Rockwell collinsi flexible digital anti-jam architecture. Proceedings of the International Technical Meeting of the Satellite Division of the Institute of Navigation, September 9-12, 2003, Portland, OR., pp: 1843-1851.

Fante, R.L. and J.J. Vaccaro, 2000. Wideband cancellation of interference in a gps receive array. Trans. Aerospace Elect. Syst., 36: 549-564.

Frost, O.L., 1972. An algorithm for linearly constrained adaptive array processing. Proc. IEEE, 60: 926-935.

Goldstein, J.S., I.S. Reed and L.L. Scharf, 1998. A multistage representation of the Wiener filter based on orthogonal projections. Trans. Inform. Theo., 44: 2943-2959.

Griffiths, L.J. and C.W. Jim, 1982. An Alternative approach to linearly constrained adaptive beamforming. Trans. Antennas Propag., 30: 27-34.

Hatke, G.F., 1998. Adaptive array processing for wideband nulling in GPS systems. Proceedings of the 32th Asilomar Conference on Signals, Systems and Computers, November 1-4, 1998, Pacific Grove, CA., USA., pp: 1332-1336.

Honig, M.L. and W. Xiao, 2001. Performance of reduced-rank linear interference suppression. Trans. Inform. Theo., 47: 1928-1946.

Honig, M.L. and J.S. Goldstein, 2002. Adaptive reduced-rank interference suppression based on the multistage wiener filter. Trans. Commun., 50: 986-994.

Mass, J.D., 1986. A selected bibliography on adaptive antenna arrays. A selected bibliography on adaptive antenna arrays. 22: 781-798.

Ricks, D.C. and J.S. Goldstein, 2000. Efficient architectures for implementing adaptive algorithms. Proceedings of the Antenna Applications Symposium, September 20-22, 2000, Allerton Park, Monticello, Illinois, pp: 29-41.

Rowe, D., J. Weger and J. Walke, 2005. Integrated GPS anti-jam systems. Proceedings of the 18th International Technical Meeting of the Satellite Division of the Institute of Navigation (ION GNSS 2005), September 2005, Long Beach, CA., pp: 1-7.

Van-Veen, B.D. and K.M. Buckley, 1988. Beamforming: A versatile approach to spatial filtering. IEEE ASSP Magazine, 5: 4-24.

Vook, F.W. and R.T. Compton, 1992. Bandwidth performance of linear adaptive arrays with tapped delay-line. Trans. Aerospace Electr. Syst., 28: 901-908.